

Article

# User-BS Selection Strategy Optimization with RSSI-Based Reliability in 5G Wireless Networks

Jie Shen <sup>1,2</sup> , Yijun Hao <sup>1,2</sup>, Yuqian Yang <sup>2,3</sup> and Cong Zhao <sup>1,2,\*</sup>

<sup>1</sup> School of Mathematics and Statistics, Xi'an Jiaotong University, Xi'an 710049, China; sj19998@stu.xjtu.edu.cn (J.S.); yijunhao@stu.xjtu.edu.cn (Y.H.)

<sup>2</sup> National Engineering Laboratory for Big Data Analytics, Xi'an Jiaotong University, Xi'an 710049, China; yuqian.yang@stu.xjtu.edu.cn

<sup>3</sup> School of Computer Science and Technology, Xi'an Jiaotong University, Xi'an 710049, China

\* Correspondence: congzhao@xjtu.edu.cn

**Abstract:** Although fifth-generation (5G) wireless communication can support well a high data rate of transmission, issues such as base station (BS) failure and poor BS signals may cause serious interruption problems. This paper studies the user-BS selection strategy with received signal strength indication (RSSI)-based reliability in 5G wireless networks. First, reliability is defined on the basis of the RSSI and failure probability of the BS. The problem is modeled as a selection strategy optimization problem with BS capacity and receiving sensitivity as constraints. Second, the original problem can be transformed into a resource allocation problem with probabilistic constraints. For the situation where user distribution is known, we used dynamic programming to obtain the optimal BS selection strategy. For the situation where user distribution is unknown, starting from user trajectory data, we used the space–time density estimation method based on the Epanechnikov kernel to estimate user density and bring it into dynamic programming to obtain the optimal selection strategy. Simulation results show that our density estimation algorithm is more accurate than the commonly used density estimation algorithm. Compared with the distance-based optimization method, our RSSI-based optimization method also improved the communication signal quality under different scenarios.

**Keywords:** wireless network; selection-strategy optimization; RSSI; dynamic programming; space–time density estimation



**Citation:** Shen, J.; Hao, Y.; Yang, Y.; Zhao, C. User-BS Selection Strategy Optimization with RSSI-Based Reliability in 5G Wireless Networks. *Appl. Sci.* **2022**, *12*, 6082. <https://doi.org/10.3390/app12126082>

Academic Editors: Yang Yue, Runzhou Zhang, Hao Feng, Zheda Li, Lin Zhang and Dawei Ying

Received: 20 May 2022

Accepted: 14 June 2022

Published: 15 June 2022

**Publisher's Note:** MDPI stays neutral with regard to jurisdictional claims in published maps and institutional affiliations.



**Copyright:** © 2022 by the authors. Licensee MDPI, Basel, Switzerland. This article is an open access article distributed under the terms and conditions of the Creative Commons Attribution (CC BY) license (<https://creativecommons.org/licenses/by/4.0/>).

## 1. Introduction

With the continuous increase in the number of network users, people's requirements for network operation speed and stability are also increasing, and the emergence of 5G wireless communication technology can effectively meet current users' comprehensive needs for network and device communication. It can also greatly enhance the user's service experience [1]. In order to meet the ever-increasing demand for data services, wireless communication networks using the 30–300 GHz millimeter-wave frequency band have become an indispensable part of the 5G communication system [2,3]. However, millimeter wave transmission is still affected by severe signal attenuation and congestion, which requires a sophisticated BS deployment plan for heterogeneous cellular networks [4]. In addition, in order to combat high path loss, 5G wireless BSs are usually densely deployed. Different from the fixed signal transmission paths in wired networks, signals have different transmission paths in wireless networks due to different user-BS connection strategies. Especially when users move, even the connectivity between users and 5G wireless BSs rapidly changes. Therefore, how to associate users with BSs to ensure the reliability of communication as much as possible is another key issue for 5G wireless networks [5], and this is the key object of this paper.

The user-BS connection strategy is an important issue in wireless communication systems and has been extensively studied in the past few decades. In traditional cellular

systems, BSs are usually deployed to achieve seamless network coverage. Whether a user can be covered by a BS depends on the distance between them [4]. However, such a user-BS connection strategy based solely on distance is difficult to meet the high standards of 5G wireless networks [6], since distance is only from a geometric point of view and can only reflect limited information. The standard requirements of the 5G networks are quite different from 4G in terms of low latency, bandwidth, reliability, and availability [7]. In order to deal with the problems encountered in actual situations, the user-BS connection strategy mostly starts from some utility indicators such as spectral and energy efficiency, and quality of service (QoS) [8]. However, instead of being inherent properties, these utility indicators are defined by people. In addition to difficulties in obtaining, there may also exist problems such as inconsistent standards. In order to address the above problems, we need to consider a common and real indicator that can easily be obtained in practical scenarios. In addition, the above studies rarely take reliability into account, while 5G wireless networks have high requirements for reliability. Reliability is one of the most important factors of wireless network communication quality; it can not only improve user experience, but also help operators in operation and maintenance. On the basis of the above motivations, we considered modeling the user-BS connection strategy problem as an optimization problem with reliability as the optimization object.

The received signal strength indicator (RSSI) is commonly used in the communication localization field [9]. RSSI can easily be obtained from most WiFi receivers such as mobile phones, tablets, and laptops [10,11]. RSSI meets the above requirements, so we chose to optimize reliability with RSSI.

This paper studies the optimization of 5G wireless communication networks based on RSSI by rationally designing a BS-user strategy selection scheme. For the selection strategy, our goal was to maximize the communication signal quality of the overall wireless network when BS capacity and receiving sensitivity constraints are met. Since the constraint function exists in the form of an expectation function that cannot be handled by the traditional random approximation simulated annealing (SA) algorithm, we began from user distribution and considered the two cases where user distribution is known and unknown.

In the case of a given user distribution, the distribution table is used to directly derive the confidence interval at a given significance level. Random constraints are converted into general constraints, and the dynamic programming method is then used to solve the optimization problem. For the case where the user distribution is unknown, we estimated the density of users on the basis of trajectory data, and derived the dynamic programming recursion formula on the basis of the estimated density. Our main contributions are listed below:

- (1) In order to meet the high requirements for reliability in 5G wireless networks, we propose to model the user-BS selection strategy problem as an optimization problem with reliability as the object.
- (2) In view of the drawbacks in commonly used indicators, we chose to define reliability by the RSSI for the first time, which could easily be obtained in practical scenarios. Considering the time-varying nature of the user's position, we transformed the original problem into a resource allocation problem under probability constraints, and solved it with dynamic programming and the time-space density estimation method.
- (3) We conducted two comparative simulations to verify the superiority of our algorithm in terms of the density estimation effect and the reliability approach GeoLife GPS Trajectories dataset [12]. Simulation 1 showed that, under different sampling frequencies, our time-space density estimation method improved accuracy by 2.84% compared to the two-dimensional kernel density estimation method. Simulation 2 showed that, compared with the distance-based selection strategies, our RSSI-based selection strategies improved communication reliability by an average of 3.57% under the three scenarios above.

The rest of this paper is organized as follows. Section 3 presents the system model and formulates the BS-user selection strategy problem. In Section 4, the wireless BS selection-

strategy optimization problem based on identified distribution is solved by dynamic programming. The wireless BS selection-strategy optimization problem based on user trajectory is addressed in Section 5, where a time–space density estimation method is proposed. Simulation results are presented in Section 6 to illustrate the performance of the proposed time-space density estimation method under different RSSI scenarios. Lastly, Section 7 concludes this paper.

## 2. Related Work

### 2.1. User-BS Selection Strategy

User-BS selection, aiming to associate a user with a particular serving BS, is a critical procedure in wireless networks that substantially affects network performance [13]. In traditional LTE systems, the radio admission control entity is located in the radio resource control layer of the protocol stack, which decides whether a new radio-bearer admission request is admitted or rejected [14]. The distance-based user-BS selection strategy where a user chooses to associate with the nearest BS is the most prevalent. Five metrics are commonly used in user-BS selection, namely, outage/coverage probability, spectral efficiency, energy efficiency, QoS, and fairness [15]. In actual situations, one or a combination of several indicators are used. The new technologies and standards of 5G networks inevitably render ineffective the above rudimentary user-BS selection strategy and metrics, and more effective user-BS selection algorithms are needed for addressing the unique features of emerging 5G wireless networks.

Utility is widely used in the modeling of user association problems. In order to make decisions, utility quantifies the satisfaction that a particular service provides to decision makers [16]. According to the used metrics, utility considered in user association may consist of, for example, spectral efficiency [17], energy efficiency [18,19], QoS [20]. Logarithms, exponentials, and sigmoidal utility functions are used to model these properties. For studies that do not specifically discuss the selection of utility functions, it can be assumed that they use linear utility functions, that is, utility is spectral efficiency, energy efficiency, or QoS itself [21]. Game theory [22], combinatorial optimization [23], and random geometry [24] are commonly used models to solve user-BS selection strategy problems. Details are shown in Table 1.

**Table 1.** Common metrics and models for user-BS selection strategy problems.

Metrics	Spectral efficiency	[17]
	Energy efficiency	[18,19]
	QoS	[20]
Models	Game theory	[22]
	Combinatorial optimization	[23]
	Random geometry	[24]

### 2.2. RSSI-Based Optimization Model

In wireless communication networks, signal quality is an important indicator that affects communication reliability, and received signal strength (RSS) is its most important part. The majority of existing work for RSS focused on large-scale cooperative sensor network localization subject to communication constraints. To the best of our knowledge, RSS was first considered for cooperative localization in [25], where a single RSS was optimized so as to limit the number of neighboring sensors. In a recent work [26], RSS was considered for noncooperative infrastructure-based indoor positioning. However, the focus of the above study lay on the overall positioning performance in a given service area and thorough treatment on the measurement campaign, RSS modeling, model fitting and parameter calibration, signaling, and performance evaluation using real data measured from a live network.

In order to measure RSS, we have RSSI, an optional part of the transmission layer, which is one of the most important indicators used to determine the link quality and whether to increase the broadcast transmission strength [27]. Predominating RSSI models can be divided into three types: the spatial-propagation, ShadowWing, and distance-loss models. Considering the influence of complex factors such as reflection, blocking, and diffraction, the distance-loss model is more capable of reflecting the actual application environment and the closest to the true value of the distance [28].

RSSI indicates the strength of the received wireless signal, which is easily affected by the environment and has unstable characteristics. Its value gradually decreases as the distance between the terminal and the access point increases. The larger the RSSI is, the higher the signal reception strength and the better the data transmission channel are. On the other hand, the lower the RSSI is, the weaker the received signal and the worse the quality of the physical channel for data transmission are, and the probability of packet loss and bit errors during data transmission obviously increases.

RSSI calculates propagation loss by measuring the transmission power and the received power, and then uses the signal attenuation model to convert propagation loss into transmission node distance [29]. This is a low-power, low-cost ranging technology with the characteristics of low cost, less equipment, long distance, and easy access.

Due to the above advantages, RSSI is often used to solve optimization problems in wireless communication. In [30] RSSI was used to resolve the optimization problem of Bluetooth low-energy (BLE) beacon density, and the authors in [31] used RSSI to help in person tracking and monitoring in industrial environments. However, most of the existing RSSI-based optimization models mainly focused on indoor localization and rarely applied it to other scenarios.

In this paper, we define the overall reliability of the wireless network by the RSSI, which can easily be obtained in the real-world scenario, together with the failure probability of the BS, and model the problem as a selection strategy optimization problem with reliability as the optimization goal.

### 3. System Model and Problem Formulation

We considered a wireless network with  $N$  BSs serving a group of users in a 2-dimensional geometry. We used  $R_{BS}$  to denote the invalid probability of each BS, and  $N_{BS}$  to denote the number of connection restrictions for each BS. Let  $\mathcal{S}$  denote the set of all BS selection strategies, from which users choose the appropriate strategy  $s \in \mathcal{S}$ . We used  $x$  to denote the position coordinates of UEs, and then  $s(x)$  can be expressed in detail as  $(s_1(x), s_2(x), \dots, s_N(x))$ . Such a selection strategy means the probability that the user chooses to connect to BS  $i$  at location  $x$  is  $s_i(x)$ , and we have  $s_i(x) \in [0, 1]$  together with  $\sum_{i=1}^N s_i(x) = 1$ . Our optimization goal was to maximize the quality of the communication signal, so we define the reliability of the communication signal from the perspective of reliability modeling.

Throughout this paper,  $\mathbb{P}[A]$  denotes the probability of event  $A$ ,  $d_i(x)$  denotes the distance between BS  $i$  and user location  $x$ ,  $R_{BS}(i)$  denotes the probability that BS  $i$  is invalid,  $s$  denotes the selection strategy,  $\mathbb{E}[\cdot]$  denotes the expectation operator,  $\alpha$  denotes the given significance level, and  $\lambda$  denotes the confidence interval.

#### 3.1. Reliability Modeling

The main objective of reliability modeling is to express the reliability of a given system in terms of the reliability measures of its constituent components. Consider a system  $Y$  that consists of  $n$  components. Each component can only have two distinct states: it can either be functional or be off. Let binary variable  $\pi_i$  be the state indicator of component  $i$  as follows:

$$\pi_i = \begin{cases} 1, & \text{if component } i \text{ is on,} \\ 0, & \text{if component } i \text{ is off.} \end{cases} \quad (1)$$

A state of system  $Y$  is a description of the states of all its components; hence,  $\pi = \{\pi_i\}$  for  $i = 1, \dots, n$ . Let  $\Pi$  be the set of all possible states of  $Y$ . The structural function of  $Y$ , denoted by  $f(\pi)$ , is a binary function that indicates whether the system is working under a given state according to the following equation:

$$f(\pi) = \begin{cases} 1, & Y \text{ is functional,} \\ 0, & Y \text{ has failed.} \end{cases} \quad (2)$$

On the basis of the above definitions, the reliability of  $Y$ , denoted by  $R(Y)$ , can be calculated using the following equation:

$$R(Y) = \mathbb{P}[f(\pi) = 1] = \sum_{\pi \in \Pi} f(\pi) \mathbb{P}[\pi]. \quad (3)$$

### 3.2. RSSI

RSSI is a method of receiving signal strength indicating ranging. In an actual application environment, since a wireless signal is affected by various obstacles, reflections, multipath propagation, temperature, and propagation mode, electromagnetic wave transmission loss conforms to the lognormal shadow model, which can be described by the modified path-loss model [29]:

$$PL(d) = PL(d_0) + 10n \log_{10}\left(\frac{d}{d_0}\right) + X_\sigma, \quad (4)$$

where  $PL(d)$  is the loss after signal propagation distance  $d$ ,  $PL(d_0)$  is the loss after signal propagation distance  $d_0$ ,  $n$  is the propagation factor (usually  $2 \sim 5$ ), and  $X_\sigma$  is the shielding factor that is a Gaussian random noise variable with mean 0 and variance  $\alpha$ .

$PL(d_0)$  in (4) can be calculated by the outdoor radio free space propagation model. The free space propagation model [32] is:

$$PL(d_0) = 32.44 + 10n \log_{10}(d) + 10n \log_{10}(f_c), \quad (5)$$

where  $f_c$  is the frequency of the propagated signal, and  $d$  is the distance between the sending and receiving nodes; usually,  $d_0 = 1$  m. Our approach is not restricted by this specific formula and it can be straightforwardly extended to any path-loss forms.

The signal strength of the anchor node received by the unknown node is:

$$RSSI(d) = P_s + P_a - PL(d), \quad (6)$$

where  $P_s$  is the transmitting power of the node signal,  $P_a$  is the antenna gain, and  $PL(d)$  is the loss after signal propagation distance  $d$ . According to Formulas (4)–(6), the distance can be calculated.

In the WINNERII C2 model [33] that simulates the wireless channel of the cellular connection in take 5G network environment, the path-loss value at distance  $d$  from the urban macrocell base station can be expressed as:

$$PL(d) = 27 + 22.7 \log_{10}(d) + 20 \log_{10}(f_c) + X_\sigma. \quad (7)$$

### 3.3. Optimization Model with RSSI-Based Reliability

The higher the received signal strength is, the more reliable the connection is. Combined with failure probability  $R_{BS}(i)$  and  $\mathbb{P}[\pi]$  in (3), the reliability of the user at location  $x$ ,  $R(s, x, R_{BS})$ , can be expressed by selecting strategies  $s$ ,  $x$ , and  $R_{BS}$  :

$$R(s, x, R_{BS}) = \sum_{i=1}^N s_i(x) RSSI(d_i(x)) (1 - R_{BS}(i)). \quad (8)$$

Combining Equation (8) with user distribution, the overall reliability of wireless side  $R_w$ , can be calculated as:

$$\begin{aligned}
 R_w &= \iint R(s, x, R_{BS})f(x)dx \\
 &= \iint \sum_{i=1}^N s_i(x)(1 - R_{BS}(i))RSSI(d_i(x))f(x)dx \\
 &= \sum_{i=1}^N \iint s_i(x)(1 - R_{BS}(i))RSSI(d_i(x))f(x)dx.
 \end{aligned} \tag{9}$$

The overall optimization problem is:

$$\max_{s \in \mathcal{S}} \sum_{i=1}^N \iint s_i(x)(1 - R_{BS}(i))RSSI(d_i(x))f(x)dx. \tag{10}$$

BS capacity refers to the number of channels that should be configured for a base station or a cell. In large cities and megacities, due to the rapid growth of users, each BS should be equipped with as many available channels as possible. Therefore, BS capacity becomes user capacity calculated by the number of channels. When there are too many users connected to the same BS, this leads to a decrease in communication quality and reduced reliability. Therefore, the expected number of users connected to each BS  $i$  cannot exceed the limit of the number of connections of BS capacity  $N_{BS}(i)$ . For each BS  $i$ , the probability of a user connecting to it can be expressed as  $\iint s_i(x)f(x)dx$ , so the capacity condition for  $M$  users can be expressed as:

$$M \iint s_i(x)f(x)dx \leq N_{BS}(i), \tag{11}$$

for  $i = 1, 2, \dots, N$ .

Receiving sensitivity refers to the minimal received signal strength with which the receiver can correctly take out the useful signal, which means that the RSSI must be greater than receiving sensitivity  $SEN$ :

$$RSSI > SEN. \tag{12}$$

$SEN$  [34] can be expressed as:

$$SEN = 10 \log_{10}(KT0) + 10 \log_{10}(BW) + NF + SNR_{min}. \tag{13}$$

where,  $10 \log_{10}(KT0)$  represents that the noise floor at a room temperature of 25 °C is  $-174$  dBm,  $BW$  refers to bandwidth,  $NF$  is the noise figure of the system that generally refers to the noise figure of the first low noise amplifier, and  $SNR_{min}$  is the minimal signal-to-noise ratio (SNR) requirement of the receiver. Similar to RSSI, the above approach is not restricted by this specific formula and can be straightforwardly extended to any sensitivity forms.

Taking a gNodeB BS of 5G NR with 20 MHz bandwidth as an example, the  $SEN$  of gNodeB is:

$$\begin{aligned}
 SEN &= -174 + 10 \log_{10}(19.08 \times 10^6) + 6 + (-1) \\
 &= -96.2,
 \end{aligned} \tag{14}$$

where  $BW = 20$  MHz, and the actual bandwidth occupied by the business is 19 MHz;  $NF = 6$  dB for the system.  $NF$  here is the insertion loss before the first-level LNA and the noise coefficient  $NF$  of the LNA itself,  $SNR_{min} = -1$  dB.

According to the RSSI formula [35]:

$$d = d_0 10^{\frac{P_a + P_s - PL(d_0)}{10n}} 10^{-\frac{1}{10n} RSSI(d)}, \tag{15}$$

so  $RSSI(d_i(x)) > \text{Sensitivity}$  can be transformed into

$$d_i(x) < D = d_0 10^{\frac{P_i - PL(d_0)}{10n}} 10^{-\frac{1}{10n} SEN}, \tag{16}$$

which means that signal effective range  $C_i$  is given to any BS  $i$ , which satisfies that  $\forall x \in C_i, d_i(x) < D$ , and  $D$  represents the maximal signal connection distance. Therefore, the optimization problem under constraints can be expressed as:

$$s_i(x) = 0, \quad \text{for } x \notin C_i. \tag{17}$$

On the basis of Equation (10), considering BS capacity (11) and SEN (17) constraints at the same time, the optimization problem can be expressed as follows:

$$\max_{s \in S} R_w, \tag{18}$$

$$s.t. \begin{cases} M \iint s_i(x) f(x) dx \leq N_{BS}(i), \\ s_i(x) = 0, \end{cases} \tag{19}$$

for  $i = 1, 2, \dots, N$  and  $x \notin C_i$ .

#### 4. Wireless BS Selection-Strategy Optimization Based on Identified Distribution

First, the optimization problem is simplified. According to the calculation formula of  $RSSI(d)$ ,  $RSSI(d_i(x))$  is negatively correlated with  $\log_{10} d_i(x)$ , so original optimization Problem (18) can be simplified to

$$\begin{aligned} & \min_{s \in S} \iint \sum_{i=1}^N s_i(x) R_{BS}(i) \log_{10} d_i(x) f(x) dx \\ & = \min_{s \in S} \sum_{i=1}^N \iint s_i(x) R_{BS}(i) \log_{10} d_i(x) f(x) dx. \end{aligned} \tag{20}$$

The actual optimization objective of the above optimization problem is functional  $s$  instead of variable  $x$ . The general idea of finding the extreme value of a functional is to construct a Lagrangian functional according to the Lagrangian multiplier theorem and then set the Frechet derivative of the Lagrangian functional to zero.

Assuming a uniform distribution and that  $s_i(x)$  is fixed for all  $x$  locations, the optimization function is set to be:

$$f(s) = \sum_{i=1}^N \iint_C s_i R_{BS}(i) \log_{10} d_i(x) \frac{1}{A_C} dx. \tag{21}$$

with constraints:

$$\begin{aligned} g_i(s) &= M \iint s_i(x) f(x) dx - N_{BS}(i) \leq 0, \\ & 1 - \sum_{i=1}^N s_i(x) = 0, \end{aligned} \tag{22}$$

for  $i = 1, 2, \dots, N$  and  $x \notin C_i$ , where  $C = \cup_{i=1}^N C_i$ ,  $A_C$  represents the area of the region  $C$ . According to the Lagrangian multiplier theorem, the Lagrangian functional is:

$$L(s, \alpha, \beta) = f(s) + \sum_{i=1}^N \alpha_i g_i(s) + \beta(1 - \sum_{i=1}^N s_i(x)). \tag{23}$$

The Frechet derivative operator  $L$  of Formula (23) is calculated, and KKT conditions (24)–(27) are solved:

$$\nabla_{s_i} L(s, \alpha, \beta) = 0, \tag{24}$$

$$\alpha_i g_i(s) = 0, \tag{25}$$

$$\alpha_i > 0, \tag{26}$$

$$1 - \sum_{i=1}^N s_i(x) = 0, \tag{27}$$

Then, we can obtain  $s_i = N_{BS}(i)/N$ .

The above method can only be applied to simple functionals. For more complex functionals, the commonly used functional optimization methods are variational methods and optimal control.

Variational method is a branch of mathematics developed at the end of the 17th century. It is a field of mathematics dealing with functions as opposed to ordinary calculus dealing with functions of numbers. The Euler–Lagrange (E–L) equation is the key theorem of the variational method that corresponds to the critical point of the functional. The E–L equation is only a necessary condition for the functional to have extreme values, but not sufficient. That is, when the functional has extreme values, the E–L equation holds.

Classical variational theory can only solve the problem of unconstrained control, but most of the problems in engineering practice are control-constrained. Therefore, modern variational theory with optimal control as the research object appeared. Optimal control refers to seeking a control under given constraint conditions to allow for the given system performance index reach the maximal (or minimal) value. The main methods to solve the optimal control problem are the classical variational method, the maximal-value principle, and dynamic programming.

The simplest form of variational method for a functional is:

$$J[y(x)] = \int_{x_1}^{x_2} F(x, y(x), y'(x)) dx. \tag{28}$$

In our optimization problem,  $F$  only depends on  $y$  and with no  $y'$ ; at this time,  $F_y \equiv 0$ , so Euler equation  $F_y(x, y) = 0$  or  $F_y(y) = 0$ . This is a functional equation whose solution does not contain any constants. The solution of this function usually does not meet the boundary conditions, and the variational problem has no solution. It is difficult to directly calculate it through mathematical methods, so we attempted to use the most advanced method, optimal control algorithms, which combines modern theoretical ideas to help in solving problems such as dynamic programming, which is an efficient mathematical method for the study and optimization of multistage sequential decision-making problems such as resource allocation.

#### 4.1. Unconstrained Optimization

The original problem can be regarded to be an optimal allocation problem,  $N$  processes correspond to the connection with  $N$  BSs, and the allocation object corresponds to the probability of connecting to each BS in selection strategies.

We can define

$$F_k(I) = \min_{s \in S} \sum_{i=1}^k \iint s_i(x) R_{BS}(i) \log_{10} d_i(x) f(x) dx,$$

with  $\sum_{i=1}^k s_i(x) = I$ . Next, we need to assign the connection probability of  $\sum_{i=1}^k s_i(x) = I$  to  $k + 1$  BSs, and the total probability assigned to the first  $k$  BSs is  $I - s_{k+1}(x)$ . According to the optimization principle, we have:

$$\begin{aligned}
 F_{k+1}(I) &= \min_{s \in \mathcal{S}} \sum_{i=1}^{k+1} \iint s_i(x) R_{BS}(i) \log_{10} d_i(x) f(x) dx \\
 &= \min_{s_{k+1}} [F_k(I - s_{k+1}(x)) \\
 &\quad + \iint s_{k+1}(x) R_{BS}(k+1) \log_{10} d_{k+1}(x) f(x) dx].
 \end{aligned}
 \tag{29}$$

Since the selection strategies were noncontinuous and unguided, we only needed to ensure that the selection strategy was optimal at each point to ensure that the overall selection strategy was optimal. Therefore, we could transform the original overall optimization (29) into optimizations on input node.

Given user location  $x_l$ , when the SEN and BS capacity constraints were not considered, we could first calculate distance  $d_i$  from the user to each BS  $i$ . According to dynamic programming,  $\sum_{i=1}^k s_i(x_l) = I$  was divided, and the following recurrence formula was obtained:

$$\begin{aligned}
 F_{k+1}(I) &= \min_{s \in \mathcal{S}} \sum_{i=1}^{k+1} s_i(x_l) R_{BS}(i) \log_{10} d_i(x_l) \\
 &= \min_{s_{k+1}} [F_k(I - s_{k+1}(x_l)) \\
 &\quad + s_{k+1}(x_l) R_{BS}(k+1) \log_{10} d_{k+1}(x_l)].
 \end{aligned}
 \tag{30}$$

#### 4.2. Constrained Optimization

The receiving sensitivity constraint condition is relatively simple with Formula (17). For input location  $x_l$  and calculated distance  $d_i$  to each BS  $i$ , it can be judged whether  $x_l$  is within the signal effective range  $C_i$  given by BS  $i$  or outside. Let those  $s_i$  corresponding to outside BSs be 0, which is not considered; only those BSs within the effective range of SEN distance are calculated step by step according to the above DP method.

According to Formula (11), the BS capacity constraint actually considers that the number of users connected to a certain one BS cannot exceed the limit, which can be transformed into the following form:

$$\iint s_i(x_l) Mf(x) dx = \mathbb{E}[ms_i(x_l)],
 \tag{31}$$

where  $m$  represents the user density at position  $x$ , whose density function is  $Mf(x)$ .

Corresponding to input position  $x$ , the BS capacity constraint condition needs to ensure  $\mathbb{P}[ms_i(x) < N_{BS}(i)] > 1 - \alpha$ . We have:

$$\begin{aligned}
 \mathbb{P}[ms_i(x_l) < N_{BS}(i)] &> 1 - \alpha \\
 \mathbb{P}[m < \frac{N_{BS}(i)}{s_i(x_l)}] &> 1 - \alpha \\
 \frac{N_{BS}(i)}{s_i(x_l)} &> \lambda_{1-\alpha} \\
 s_i(x_l) &< \frac{N_{BS}(i)}{\lambda_{1-\alpha}},
 \end{aligned}
 \tag{32}$$

$\lambda$  represents the confidence region of  $m$ 's distribution under  $\alpha$ , which can be obtained from the distribution table when the distribution is identified.

Adding the BS capacity constraint to the DP method, we can obtain:

$$\begin{aligned}
 F_{k+1}(I) &= \min_{s \in \mathcal{S}} \sum_{i=1}^{k+1} s_i(x_l) \cdot R_{BS}(i) \log_{10} d_i(x_l), \\
 & \text{s.t. } s_{C_i} < \frac{N_{BS}(C_i)}{\lambda_{1-\alpha}} \text{ for } i = 1, \dots, k+1 \\
 &= \min_{s_{k+1}} [F_k(I - s_{k+1}(x_l)) \\
 & \quad + s_{k+1}(x_l) R_{BS}(k+1) \log_{10} d_{k+1}(x_l)], \\
 & \text{s.t. } s_{C_{k+1}} < \frac{N_{BS}(C_{k+1})}{\lambda_{1-\alpha}}.
 \end{aligned} \tag{33}$$

According to the above analysis, the process of solving wireless BS selection-strategy optimization on the basis of identified distribution can be obtained as shown in Algorithm 1.

---

**Algorithm 1:** Wireless BS selection-strategy optimization based on identified distribution.

---

- Require:**  $x$ : user’s location;  $BS$ : BS information, including locations, reliability, and connection limit numbers;  $D$ : maximal signal connection distance;
- Ensure:**  $s$ : BS-user connection strategy;
- 1: **initialize:** Set  $s = 0$ ;
  - 2: **Step 1:** Calculate distance  $d_i$  from  $x$  to each BS  $i$ , and find BS set  $K_C$  within the signal effective range of the user SEN on the basis of (17); let  $k = N(K_C)$ .
  - 3: **Step 2:** Calculate the BS capacity constraint at position  $x$  according to (32).
  - 4: **Step 3:** Use the DP method (16) to calculate the optimal user selection strategy  $s$  under the condition of meeting the connection restriction.
  - 5: **return**  $s$
- 

First, the distance from  $x$  to each BS is calculated, and the nodes within the effective range of the signal are selected according to Formula (16). Then, the DP recursive formula in (33) is combined to optimize the user-BS selection strategy.

## 5. Wireless BS Selection-Strategy Optimization Based on User Trajectory

In view of unknown user distribution, we estimate the user density of any given location from the trajectory.

### 5.1. Trajectory Data

Effective data in the trajectory dataset mainly include space latitude and longitude coordinate data, and time data.

Most of the trajectory data density estimation methods only start from spatial data, which are commonly analyzed and visualized using the methods for home range or utilization distribution estimation [36]. However, these two concepts often only focus on the spatial distribution of the measured positions in 2D space and ignore the time series of the measurements. So, we used a time–space density estimation method to process the trajectory data.

### 5.2. Density Estimation

Kernel density estimation is a nonparametric estimation method that does not use prior knowledge about the data distribution and does not attach any assumptions to the data distribution. It is a method to study the characteristics of the data distribution from the data sample itself, which is consistent with our unknown user distribution situation. The so-called kernel density estimation is to use a smooth peak function, which is called a ‘kernel’, to fit the observed data points, thereby simulating the true probability distribution curve. Assuming that  $x_1, x_2, \dots, x_n$  are the  $n$  sample points of independent and identically

distributed  $F$ , whose probability density function is  $f$ , the kernel density can be estimated as follows:

$$f_h(x) = \frac{1}{n} \sum_{i=1}^n K_h(x - x_i) = \frac{1}{nh} \sum_{i=1}^n K\left(\frac{x - x_i}{h}\right), \quad (34)$$

where  $K(\cdot)$  is the kernel function (non-negative, integral is 1, conforms to the nature of probability density, and the mean is 0). There are many kinds of kernel functions, for example, uniform, triangular, biweight, triweight, Epanechnikov, and normal.

Commonly used kernel functions include the Gaussian and Epanechnikov kernels [37]:

$$K(x) = \frac{1}{\sqrt{2\pi}} \exp\left(-\frac{x^2}{2}\right) \text{ (Gaussian Kernel)}, \quad (35)$$

$$K(x) = \frac{3}{4}(1 - x^2)I(|x| \leq 1) \text{ (Epanechnikov Kernel)}. \quad (36)$$

We used a 3-dimensional kernel density estimation method to estimate the user density at the input location coordinate point, and selected the optimal Epanechnikov kernel in the sense of mean square error to estimate.

At the same time, we also added the automatic calculation of bandwidth  $h$  in Formula (34) according to the Scott principle of the  $d$ -dimensional space:

$$h = \sqrt{5} \cdot n^{\frac{1}{d+4}}, \quad (37)$$

where  $N$  represents the number of data.

We consider both space data and time data; first, the space–time kernel density function is estimated and then integrated into the time dimension. However, because it is impossible to accurately calculate the space–time nuclear density function, we could only use numerical methods to calculate the space–time nuclear density of the input position coordinates at these time nodes according to a certain time interval, which represents density in this time interval multiplied by the time interval and accumulated as the integration process. The specific algorithm pseudocode is shown as Algorithm 2.

---

**Algorithm 2:** Time–space density estimation.

---

**Require:** *points*: target location; *data<sub>space</sub>*: spatial data; *data<sub>ti</sub>*: time data; *d*: data dimension;

**Ensure:** *Den*: estimated density;

- 1: **initialize:** Set *Den* = 0;
- 2: Convert latitudinal and longitudinal data (*points* and *data<sub>space</sub>*) into coordinate axis data;
- 3: **if**  $d = 2$  **then**
- 4:   Use *data<sub>space</sub>* to estimate space density *Den* at *points* with kernel density estimation Formula (34) and the Epanechnikov kernel (36).
- 5: **end if**
- 6: **if**  $d = 3$  **then**
- 7:   Normalize time data *data<sub>ti</sub>*.
- 8:   **for**  $t = 0, 2, \dots, 19$  **do**
- 9:      $time = (i - 5)/10$ ;
- 10:    Use *data<sub>space</sub>* and *data<sub>ti</sub>* to estimate time–space density *den* at (*points*, *time*) with (34) and (36).
- 11:     $Den = Den + den/10$ .
- 12:   **end for**
- 13: **end if**
- 14: **return** *Den*

---

In time–space density estimation, there are two options for 2- and 3-dimensional density estimation. Two-dimensional density estimation only considers spatial data to estimate the user’s spatial kernel density. Three-dimensional density estimation considers both space and time data, first estimating the spatiotemporal kernel density function and then integrating it into the time dimension.

The overall flow of the algorithm is shown in Figure 1.

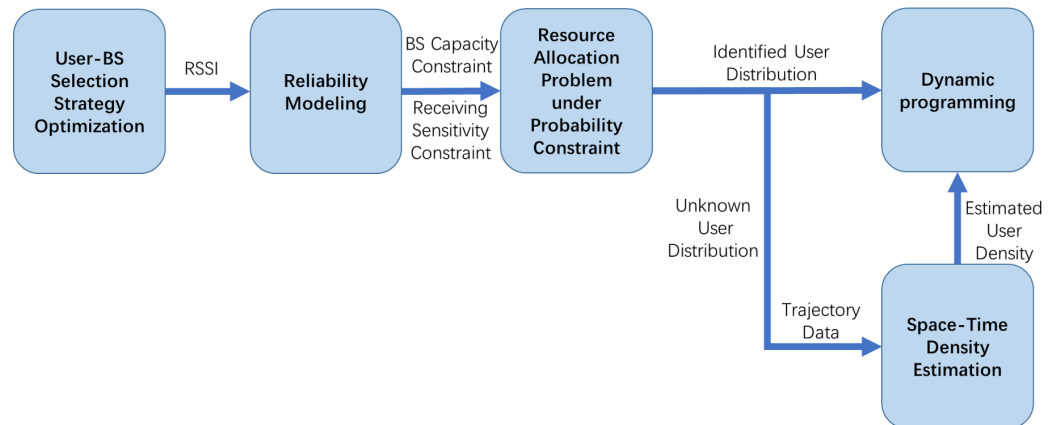


**Figure 1.** Overall flow of Algorithm 3.

On the basis of the above analysis and the time–space density estimation algorithm, the process of solving wireless BS selection-strategy optimization based on trajectory data can be obtained as Algorithm 3.

---

**Algorithm 3:** Wireless BS selection-strategy optimization based on trajectory data.

---

**Require:**  $x$ : user’s location;  $BS$ : BS information, including locations, reliability, and connection limit numbers;  $D$ : maximal signal connection distance;

**Ensure:**  $s$ : BS-user connection strategy.

- 1: **initialize:** Set  $s = 0$ ;
  - 2: **Step 1:** Calculate distance  $d_i$  from  $x$  to each BS  $i$  and find BS set  $K_C$  within the signal effective range of the user SEN on the basis of (17), let  $k = N(K_C)$ .
  - 3: **Step 2:** Calculate the density at the position of  $x$  according to the given user’s trajectory data using the time–space density estimation algorithm.
  - 4: **Step 3:** Substitute density into the the DP Formula (30) to calculate the optimal user selection strategy  $s$  under the condition of meeting the connection restriction.
  - 5: **return**  $s$
- 

First, the distance from  $x$  to each BS is calculated, and nodes within the effective range of the signal are selected according to Formula (16). Then, the user density obtained in Algorithm 2 is brought into the DP recursive formula of (30), and the user-BS selection strategy is optimized.

## 6. Performance Evaluation

We evaluated the performance of our proposed approach on the basis of the GeoLife GPS Trajectories dataset. The GeoLife GPS Trajectories dataset was assembled from the Microsoft Research Asia Geolife project by 182 users during a period of over three years (from April 2007 to August 2012). A GPS trajectory of this dataset is represented by a sequence of time-stamped points, each of which containing the information of latitude, longitude, and altitude. Of the trajectories, 91% are logged in a dense representation, e.g., every 1 to 5 s or every 5 to 10 m per point. This dataset recorded a broad range of users’ outdoor movements, including not only life routines such as going home and to work, but also some entertainment and sports activities, such as shopping, sightseeing, dining,

hiking, and cycling. Most of the data were created in Beijing, China. Figure 2 plots the trajectories of user [004] from 23 October 2008 to 5 July 2009.

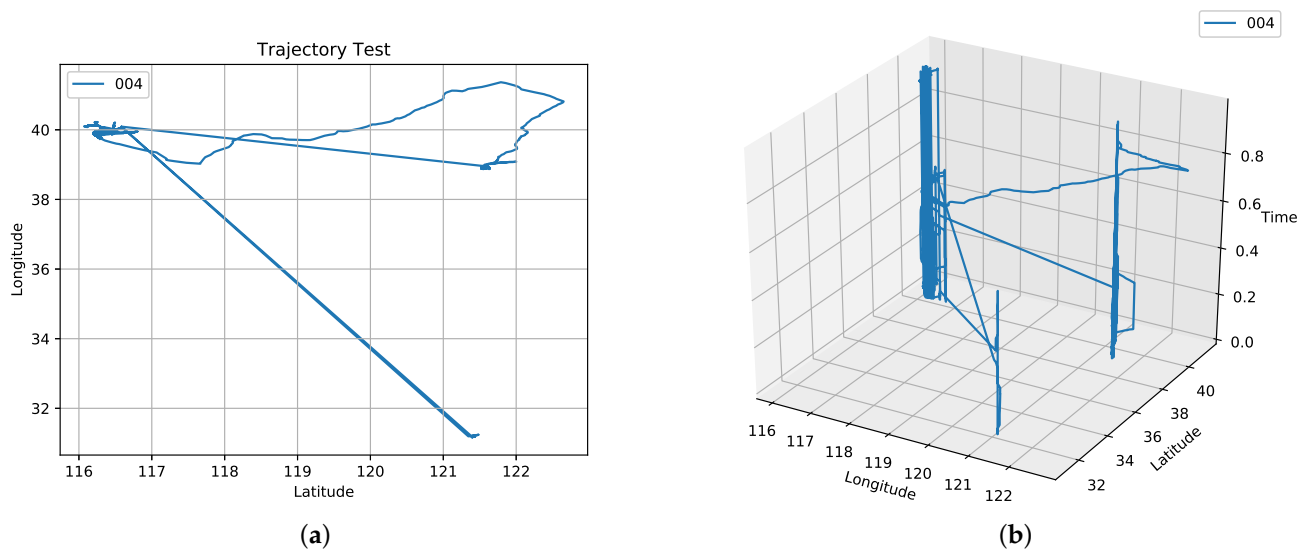


**Figure 2.** Trajectories of user [004] from 23 October 2008 to 5 July 2009. (a) Two-dimensional trajectory; (b) three-dimensional trajectory.

Figure 2a shows that the user's track coverage was relatively large, but in fact, according to the analysis of the track data and Figure 2b, the user spent most of the time within a small area in the center and had rarely traveled far away.

The reason for this difference is that Figure 2a is a two-dimensional space map that only considers the spatial scale, and ignores information in the time scale. Our algorithm considers both space and time information to estimate the density.

We conducted comparative simulations from two aspects. Simulation 1 compares the difference of the density estimation effect for 2-dimensional kernel density estimation and time-space density algorithms under different sampling frequency conditions, while Simulation 2 compares the reliabilities of RSSI- and distance-based selection strategies. Both simulations were conducted in a Python environment.

### 6.1. Comparative Simulations between Two-Dimensional Kernel Density Estimation and Time-Space Density Estimation

In order to verify the superiority of our time-space density estimation method, we conducted two comparative simulations. First, we compared our time-space density estimation method with the two-dimensional kernel density estimation method. Comparative simulations were carried out on a trajectory dataset with the same sampling time interval, together with passing the same point, and on a trajectory dataset with different sampling time intervals, together with passing the same point.

The variable between the above comparative simulations was the sampling frequency condition. We set up two simulation scenarios, A and B, which corresponded to the same sampling frequency and different sampling frequencies. Under both scenarios, we assumed that RSSI followed path-loss model  $PL(d) = 27 + 22.7 \log_{10}(d) + 20 \log_{10}(f_c)$  in the WINNERII C2 model [33]. The setups of this comparative simulation are shown in Table 2.

**Table 2.** Simulation setups for simulation under different sampling scenarios.

Path Loss		$PL(d) = 27 + 22.7 \log_{10}(d) + 20 \log_{10}(f_c)$	
Scenarios	Point	Users	Sampling Interval
Scenario A	(40.01, 116.31)	[000, 001, 002, 003, 004]	Same
Scenario B	(39.96, 116.40)	[132, 135, 163, 167, 168]	Different

In Scenario A with the same sampling time interval, we selected five user trajectories [000, 001, 002, 003, 004]. Their trajectory data were all sampled at 0.05 s, and they all passed through point (40.01, 116.31). The specific trajectory is shown in Figure 3.

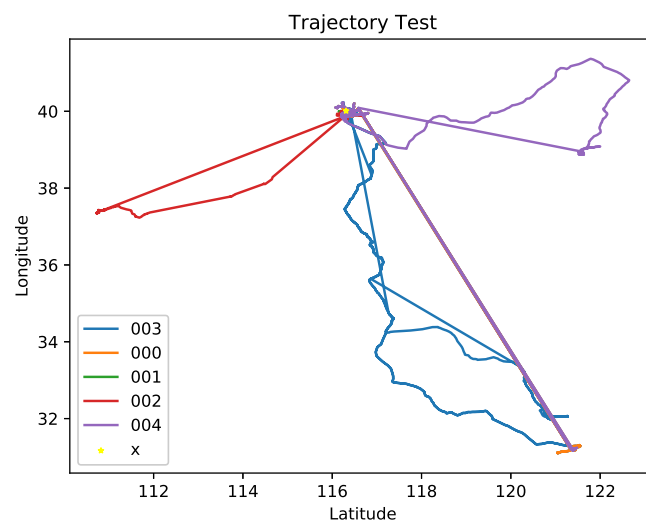


**Figure 3.** Trajectories of users [000, 001, 002, 003, 004] and point (40.01, 116.31).

The calculated 2-dimensional kernel density and time-space density at (40.01, 116.31) were 2.75 and 2.77 respectively, which are very similar.

In Scenario B with different sampling time intervals, we selected the trajectory data of five users [132, 135, 163, 167, 168]. Their data collection was rather chaotic, and the sampling time interval was not fixed. Users 135, 163, and 167 all passed through point (39.96, 116.40). The specific trajectory is shown in Figure 4.

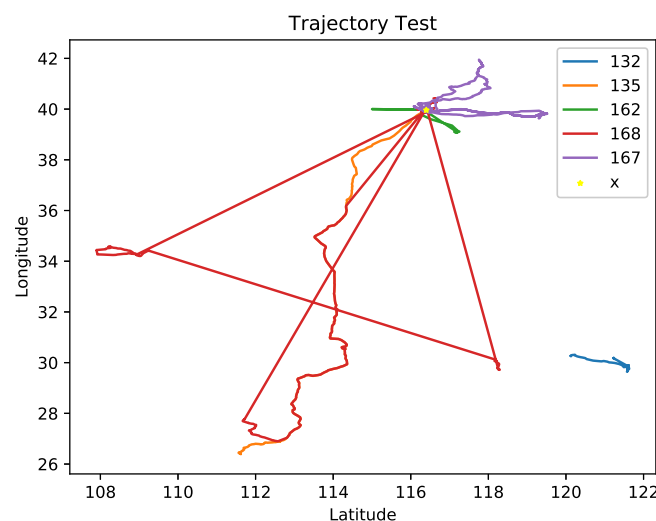


**Figure 4.** Trajectories of users [132, 135, 163, 167, 168] and point (39.96, 116.40).

The calculated two-dimensional and time-space densities at (39.96, 116.40) were 2.39 and 2.54. Simulation results at position [41, 116.33] are shown in Table 3.

**Table 3.** Simulation results for density estimation under different sampling scenarios.

Scenarios	Two-Dimensional Kernel Density Estimation	Time-Space Density Estimation	Improvements in Density Estimation Accuracy
Scenario A	2.75	2.77	0.67%
Scenario B	2.39	2.54	5.00%

Table 3 shows that, since the sampling time interval in Scenario A was the same, the influence of the time factor on the estimation of trajectory density could be ignored. In Scenario B, time-space density was significantly closer to the expected density 3 than the two-dimensional kernel density was because 2D kernel density estimation ignores the time factor. For different sampling frequencies, the density calculated at a high sampling frequency may be higher, and the density calculated at the low sampling frequency may be lower. Our time-space method first aligned the data in the time dimension, which means that it could overcome the problem of different sampling frequencies and take the effects of both time and space on density estimation into account.

#### 6.2. Comparative Simulations between RSSI-Based and Distance-Based Selection Strategy

In order to verify the improvement effect of our algorithm, we compared it with optimization on the basis of only distance rather than RSSI. In order to minimize the overall connection distance between users and BSs, the optimization object of the user-BS selection strategy optimization based on distance was set to be as follows:

$$\min_{s \in \mathcal{S}} \sum_{i=1}^N s_i(x) \cdot d_i(x), \quad (38)$$

and the constraint conditions were the same as those of the user-BS selection strategy optimization based on reliability. Comparative simulations were carried out under the conditions of known and unknown user distribution.

In order to verify the versatility of our algorithm, we also verified RSSI on the basis of different path-loss models. Path loss is presented in decibels as a function of distance, and was calculated by summing the taps in SEN domain and averaging over the measurement snapshots along the measurement run. Path loss and shadow fading are given for the urban microcell scenario (UMi), suburban macrocell scenario (SMa), and urban macrocell scenario (UMa) [33] for the frequency range of 0.45–6.0 GHz in Table 4.

**Table 4.** Path loss under different scenarios.

Scenario	Path Loss
UMi	$PL(d) = 27 + 22.7 \log_{10}(d) + 20 \log_{10}(f_c)$
SMa	$PL(d) = 27.2 + 23.8 \log_{10}(d) + 20 \log_{10}(f_c)$
UMa	$PL(d) = 25 + 26 \log_{10}(d) + 20 \log_{10}(f_c)$

In the case of the given user distribution, we considered a wireless network with 5 BSs and 10 users. The attributes of the 5 BSs were set as shown in Table 5.

**Table 5.** Simulation setup for BSs with given user distribution.

BS Serial Number	Position	$R_{BS}$	$N_{BS}$
1	[0, 0]	0.8	3
2	[5, 1]	0.8	5
3	[1, 7]	0.7	4
4	[2, 3]	0.8	5
5	[6, 2]	0.9	4

We assumed that all users followed normal distribution and the maximal signal connection distance was 8, and the user-BS selection strategies at position [5, 5] are shown in Table 6.

**Table 6.** Simulation results for reliability under given user distribution.

BS	Selection Strategy Based on RSSI	Selection Strategy Based on Distance
1	0.362	0.362
2	0	0.155
3	0	0.483
4	0.603	0
5	0.035	0
Reliability	0.565	0.540

The communication signal quality for the selection strategies based on distance and on RSSI was 0.540 and 0.565, respectively, and our RSSI-based optimization result was 4.6% higher in communication signal quality than the non-RSSI optimization result. This demonstrates that the RSSI-based method could better ensure communication reliability when user distribution is known.

In the case of unknown user distribution, we considered a wireless network with 3 BSs and 10 users. The attributes of the 3 BSs were set as shown in Table 7.

**Table 7.** Simulation setup for BSs with unknown user distribution.

BS Serial Number	Position	$R_{BS}$	$N_{BS}$
1	[39, 116.5]	0.9	3
2	[40, 116.3]	0.95	5
3	[42, 116.4]	0.85	4
4	[39, 116.3]	0.7	5
5	[40, 116.5]	0.9	4

We selected ten user trajectories [000, 001, 002, 003, 004, 005, 006, 007, 008, 009]. Simulation results at position [41, 116.33] are shown in Table 8 and Figure 5.

**Table 8.** Simulation results for reliability under different scenarios.

Scenarios	Reliability Based on RSSI	Reliability Based on Distance	Improvements in Reliability
UMi(B1)	1.990	1.943	2.4%
SMa(C1)	1.897	1.804	5.2%
UMa(C2)	1.788	1.734	3.1%

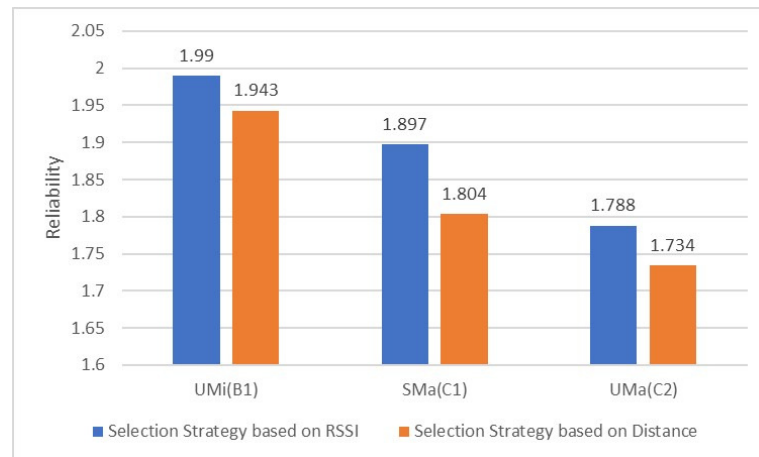


**Figure 5.** Comparison chart for simulation results under different scenarios.

Simulation results show that the reliability of the selection strategy based on RSSI was 3.6% higher on average than that of the selection strategy based on distance in the UMi, SMa, and UMa scenarios. This demonstrates that RSSI could reflect more information with the user-BS selection strategy under both user-known and user-unknown cases, which means that our algorithm is more effective than traditional distance-based algorithms in common scenarios due to the better fulfilment of the high requirements for reliability in 5G wireless networks.

## 7. Conclusions

In this paper, we presented a user-BS connection strategy optimization method based on RSSI to maximize the overall communication signal quality of 5G wireless networks. The original problem is a functional optimization problem that is difficult to solve under nonideal conditions. Therefore, we transformed it into a resource allocation problem with random constraints based on RSSI, and solved it with the DP method and space–time density estimation. Simulation results show that, compared with the estimation of the 2-dimensional kernel density method that only considers spatial data, our time–space density could simultaneously imply the information in the space and time dimensions, and solve the problems caused by random sampling frequency with an improvement of 2.84% in density estimation accuracy. At the same time, compared with the distance-based method, our RSSI-based optimization method improved the communication signal quality by an average of 3.57% under different RSSI path-loss models.

In fact, there are other factors in the reliability modeling of complex systems, such as remaining life, series, parallel connections, and the bridging model that may fit with the reliability model of 5G wireless networks. In our future work, we are focusing on the impact of the above factors on the reliability of 5G wireless networks.

**Author Contributions:** Conceptualization, J.S. and Y.Y.; data curation, J.S.; formal analysis, J.S. and Y.H.; investigation, J.S.; methodology, J.S. and Y.Y.; supervision, Y.Y. and C.Z.; validation, Y.H. and C.Z.; visualization, J.S.; writing—original draft preparation, J.S.; Writing review editing, Y.H. and C.Z. All authors have read and agreed to the published version of the manuscript.

**Funding:** This research was supported in part by the National Key Research and Development Program of China under Grant 2020YFA0713900; the National Natural Science Foundation of China under Grants 61772410, 61802298, 62172329, U1811461, U21A6005, 11690011, and the China Postdoctoral Science Foundation under Grants 2020T130513, 2019M663726.

**Institutional Review Board Statement:** Not applicable.

**Informed Consent Statement:** Not applicable.

**Data Availability Statement:** Not applicable.

**Conflicts of Interest:** The authors declare no conflict of interest.

## References

1. Tsumachi, N.; Ohseki, T.; Yamazaki, K. Base Station Selection Method for RAT-Dependent TDOA Positioning in Mobile Network. In Proceedings of the 2021 IEEE Radio and Wireless Symposium (RWS), San Diego, CA, USA, 17–22 January 2021; pp. 119–122. [\[CrossRef\]](#)
2. Boccardi, F.; Heath, R.W.; Lozano, A.; Marzetta, T.L.; Popovski, P. Five disruptive technology directions for 5G. *IEEE Commun. Mag.* **2014**, *52*, 74–80. [\[CrossRef\]](#)
3. Xiao, M.; Mumtaz, S.; Huang, Y.; Dai, L.; Li, Y.; Matthaiou, M.; Karagiannidis, G.; Björnson, E.; Yang, K.; Chih-Lin, I.; et al. Millimeter wave communications for future mobile networks. *IEEE J. Sel. Areas Commun.* **2017**, *35*, 1909–1935. [\[CrossRef\]](#)
4. Zhao, N.; Liang, Y.C.; Niyato, D.; Pei, Y.; Wu, M.; Jiang, Y. Deep reinforcement learning for user association and resource allocation in heterogeneous cellular networks. *IEEE Trans. Wirel. Commun.* **2019**, *18*, 5141–5152. [\[CrossRef\]](#)
5. Andrews, J.G.; Buzzi, S.; Choi, W.; Hanly, S.V.; Lozano, A.; Soong, A.C.; Zhang, J.C. What will 5G be? *IEEE J. Sel. Areas Commun.* **2014**, *32*, 1065–1082. [\[CrossRef\]](#)
6. Dai, Y.; Xu, D.; Maharjan, S.; Zhang, Y. Joint computation offloading and user association in multi-task mobile edge computing. *IEEE Trans. Veh. Technol.* **2018**, *67*, 12313–12325. [\[CrossRef\]](#)
7. Esmaily, A.; Kravevska, K. Small-scale 5g testbeds for network slicing deployment: A systematic review. *Wirel. Commun. Mob. Comput.* **2021**, *2021*, 6655216. [\[CrossRef\]](#)
8. Mei, W.; Zhang, R. Performance analysis and user association optimization for wireless network aided by multiple intelligent reflecting surfaces. *IEEE Trans. Commun.* **2021**, *69*, 6296–6312. [\[CrossRef\]](#)
9. Hoang, M.T.; Yuen, B.; Dong, X.; Lu, T.; Westendorp, R.; Reddy, K. Recurrent neural networks for accurate RSSI indoor localization. *IEEE Internet Things J.* **2019**, *6*, 10639–10651. [\[CrossRef\]](#)
10. Liu, C.; Fang, D.; Yang, Z.; Jiang, H.; Chen, X.; Wang, W.; Xing, T.; Cai, L. RSS distribution-based passive localization and its application in sensor networks. *IEEE Trans. Wirel. Commun.* **2016**, *15*, 2883–2895. [\[CrossRef\]](#)
11. Hao, C.; Zhang, Y.; Wei, L.; Tao, X.; Ping, Z. ConFi: Convolutional Neural Networks Based Indoor Wi-Fi Localization Using Channel State Information. *IEEE Access* **2017**, *5*, 18066–18074. [\[CrossRef\]](#)
12. Li, Q.; Zheng, Y.; Xie, X.; Chen, Y.; Liu, W.; Ma, W.Y. Mining user similarity based on location history. In Proceedings of the 16th ACM SIGSPATIAL International Conference on Advances in Geographic Information Systems, Irvine, CA, USA, 5–7 November 2008; pp. 1–10. [\[CrossRef\]](#)
13. Gatzianas, M.; Mesodiakaki, A.; Kalfas, G.; Pleros, N.; Moscatelli, F.; Landi, G.; Ciulli, N.; Lossi, L. Offline Joint Network and Computational Resource Allocation for Energy-Efficient 5G and beyond Networks. *Appl. Sci.* **2021**, *11*, 10547. [\[CrossRef\]](#)
14. Wannstrom, J. *LTE-Advanced*; Third Generation Partnership Project (3GPP): Valbonne, France, 2013.
15. Liu, D.; Wang, L.; Chen, Y.; Elkashlan, M.; Wong, K.K.; Schober, R.; Hanzo, L. User association in 5G networks: A survey and an outlook. *IEEE Commun. Surv. Tutor.* **2016**, *18*, 1018–1044. [\[CrossRef\]](#)
16. Alizadeh, A.; Vu, M. Load balancing user association in millimeter wave MIMO networks. *IEEE Trans. Wirel. Commun.* **2019**, *18*, 2932–2945. [\[CrossRef\]](#)
17. Feng, M.; Mao, S.; Jiang, T. Joint Frame Design, Resource Allocation and User Association for Massive MIMO Heterogeneous Networks with Wireless Backhaul. *IEEE Trans. Wirel. Commun.* **2017**, *17*, 1937–1950. [\[CrossRef\]](#)
18. Zhou, T.; Nan, J.; Dong, Q.; Liu, Z.; Li, C. Joint Cell Selection and Activation for Green Communications in Ultra-Dense Heterogeneous Networks. In Proceedings of the 2017 IEEE International Conference on Computational Science and Engineering (CSE) and IEEE International Conference on Embedded and Ubiquitous Computing (EUC), Guangzhou, China, 21–24 July 2017. [\[CrossRef\]](#)
19. Zola, E.; Kassler, A.J.; Kim, W. Joint User Association and Energy Aware Routing for Green Small Cell mmWave Backhaul Networks. In Proceedings of the 2017 IEEE Wireless Communications and Networking Conference (WCNC), San Francisco, CA, USA, 19–22 March 2017; pp. 1–6. [\[CrossRef\]](#)
20. Tan, J.; Xiao, S.; Han, S.; Liang, Y.C.; Leung, V. QoS-Aware User Association and Resource Allocation in LAA-LTE/WiFi Coexistence Systems. *IEEE Trans. Wirel. Commun.* **2019**, *18*, 2415–2430. [\[CrossRef\]](#)
21. Zhang, H.; Huang, S.; Jiang, C.; Long, K.; Leung, V.C.; Poor, H.V. Energy efficient user association and power allocation in millimeter-wave-based ultra dense networks with energy harvesting base stations. *IEEE J. Sel. Areas Commun.* **2017**, *35*, 1936–1947. [\[CrossRef\]](#)
22. Luo, Q.; Su, G.; Lin, X.; Chen, B.; Dai, M.; Wang, H. A Stable Matching Game for User Association in Heterogeneous Cellular Networks. In Proceedings of the 2019 IEEE 5th International Conference on Computer and Communications (ICCC), Chengdu, China, 6–9 December 2019; pp. 1098–1102. [\[CrossRef\]](#)
23. Soleymani, B.; Zamani, A.; Rastegar, S.H.; Shah-Mansouri, V. RAT selection based on association probability in 5G heterogeneous networks. In Proceedings of the 2017 IEEE Symposium on Communications and Vehicular Technology (SCVT), Leuven, Belgium, 14 November 2017; pp. 1–6. [\[CrossRef\]](#)
24. Afshang, M.; Dhillon, H.S. Poisson cluster process based analysis of HetNets with correlated user and base station locations. *IEEE Trans. Wirel. Commun.* **2018**, *17*, 2417–2431. [\[CrossRef\]](#)

25. Giorgetti, G.; Gupta, S.; Manes, G. Optimal RSS threshold selection in connectivity-based localization schemes. In Proceedings of the 11th International Symposium on Modeling Analysis and Simulation of Wireless and Mobile Systems, MSWiM 2008, Vancouver, BC, Canada, 27–31 October 2008. [[CrossRef](#)]
26. Feng, Y.; Zhao, Y.; Gunnarsson, F. Proximity report triggering threshold optimization for network-based indoor positioning. In Proceedings of the 2015 18th International Conference on Information Fusion (Fusion), Washington, DC, USA, 6–9 July 2015.
27. Ghatak, G. On the Placement of Intelligent Surfaces for RSSI-Based Ranging in Mm-Wave Networks. *IEEE Commun. Lett.* **2021**, *25*, 2043–2047. [[CrossRef](#)]
28. Sadowski, S.; Spachos, P. Rssi-based indoor localization with the internet of things. *IEEE Access* **2018**, *6*, 30149–30161. [[CrossRef](#)]
29. Marks, M.; Niewiadomska-Szynkiewicz, E. Localization based on stochastic optimization and RSSI measurements. In Proceedings of the ACM/IEEE International Conference on Information Processing in Sensor Networks, Stockholm, Sweden, 12–16 April 2010; p. 402. [[CrossRef](#)]
30. Sadowski, S.; Spachos, P. Optimization of BLE beacon density for RSSI-based indoor localization. In Proceedings of the 2019 IEEE International Conference on Communications Workshops (ICC Workshops), Shanghai, China, 20–24 May 2019; pp. 1–6. [[CrossRef](#)]
31. Aravinda, P.; Sooriyaarachchi, S.; Gamage, C.; Kottege, N. Optimization of RSSI based indoor localization and tracking to monitor workers in a hazardous working zone using Machine Learning techniques. In Proceedings of the 2021 International Conference on Information Networking (ICOIN), Jeju Island, Korea, 13–16 January 2021; pp. 305–310. [[CrossRef](#)]
32. Rappaport, T.S. *Wireless Communications: Principles and Practice*; Horwood Publishing Limited: Chichester, UK, 2002.
33. Heino, P.; Meirilä, J.; Kysti, P.; Hentil, L.; Narandzic, M. CP5-026 WINNER+ D5.3 v1.0 WINNER+ Final Channel Models. *Waseda Commercial Review*, 30 January 2010. Available online: <https://docplayer.net/34577643-D5-3-winner-final-channel-models.html> (accessed on 13 June 2022).
34. Yuan, M.; Xu, W.; Zhi, Q.; Poor, H.V. Data-Driven Measurement of Receiver Sensitivity in Wireless Communication Systems. *IEEE Trans. Commun.* **2019**, *67*, 3665–3676. [[CrossRef](#)]
35. Dieng, N.A.; Chaudet, C.; Charbit, M.; Toutain, L.; Meriem, T.B. Experiments on the RSSI as a Range Estimator for Indoor Localization. In Proceedings of the 2012 5th International Conference on New Technologies, Mobility and Security (NTMS), Istanbul, Turkey, 7–10 May 2012. [[CrossRef](#)]
36. Zou, Y.; Chen, Y.; He, J.; Pang, G.; Zhang, K. 4D time density of trajectories: Discovering spatiotemporal patterns in movement data. *ISPRS Int. J. Geo-Inform.* **2018**, *7*, 212. [[CrossRef](#)]
37. Wglarczyk, S. Kernel density estimation and its application. *ITM Web Conf.* **2018**, *23*, 00037. [[CrossRef](#)]